Dynamic Analysis and Experiment Methods for a Generic Space Station Model

W. Keith Belvin*
NASA Langley Research Center, Hampton, Virginia
and
Harold H. Edighoffer†
Edighoffer, Inc., Newport News, Virginia

Modal vibration tests in conjunction with finite-element analysis were used to characterize a generic dynamic model. The model consisted of five substructures to simulate the multibody, low-frequency nature of large space structures. Static tests were used to refine the substructure analytical models prior to full assemblage analysis. The effects of a cable suspension system were analyzed using a prestressed vibration analysis. Coupling between a cable suspension mode and model bending mode was found to be influenced by the distance from the model center of gravity to the cable-to-model attachment location. A damping characterization method using noncontacting exciters was used to measure the amplitude-dependent damping. Frequency and damping measurements in ambient air and at near-vacuum conditions were made. Ambient air decreased vibration frequencies by an average 3.1% and increased the modal damping by an average 28% in the generic model.

Nomenclature

C/C_c = critical damping ratio
f_1 = fundamental frequency, Hz
g = acceleration due to gravity
I = model rotational inertia
ℓ_1 = suspension cable length
ℓ_2 = distance from model center of gravity to cable-to-model attachment location
m = vibration cycle number
M = model mass
X_0 = initial vibration amplitude
X_m = vibration amplitude of the mth cycle
$\theta_1, \ddot{\theta}_1$ = cable rotation and rotational acceleration (Fig. 13)
$\theta_2, \ddot{\theta}_2$ = model rotation and rotational acceleration (Fig. 13)
ω = circular frequency, $2\pi f$

Introduction

LARGE space systems require accurate dynamic analysis to insure that structural vibrations do not adversely impact performance. Verification of analysis models is typically performed during development phases using a limited series of tests. Of particular interest to the structural dynamicist are the natural frequencies, mode shapes, and damping characterizing the structure. Modal vibration tests are frequently used to determine the modes and frequencies occurring over some frequency range of interest. The predicted and experimental frequencies are compared and the analysis refined until the error between prediction and test falls within specified tolerances.

Several difficulties occur using the aforementioned method of analytical model verification. First, the best rationale for refining the analytical models to match test data is not clear. References 1-3, among others, propose using automated computer methods to refine analysis models based on measured eigenvalues and eigenvectors. Unfortunately, the accurate measurement of eigenvectors of complex built-up structures is difficult. A second area of difficulty involves the suspension systems that must be used in ground vibration tests. These systems only approximate the free-free boundary conditions of orbiting spacecraft. Some work exists in the literature on assessing the influence of suspension systems[4,5]; however, no method for completely simulating free-free boundary conditions during ground vibration testing has been documented. Another area of concern for analysis verification using test data is the inability to test some large flexible structures. Full-scale substructures and scale model testing must then be relied on to refine the analytical models.

The focus of the present paper is to document the methods used on a generic model for dynamic analytical model verification. The finite-element analysis and modal vibration tests used to characterize the experimental model are presented. A description of static tests used to refine the analytical models in physical coordinates is given. Mode coupling due to suspension system effects and a method to extract nonlinear damping are presented. In addition, ambient air effects on the model frequency and damping are shown using test data obtained at atmospheric and near-vacuum pressures.

Generic Dynamic Model

Numerous structural designs for a space station have been suggested. Common among many designs is the use of cylindrical modules for habitation, solar array panels for power generation, and radiator panels for heat dissipation. These common elements are interconnected to form an integral orbiting platform. The study reported herein used a generic model, designed prior to the space station reference configuration selection,[6] to simulate the multibody, low-frequency nature of scaled space station models.

The generic model, shown in Fig. 1, consists of a cylindrical habitation module, two solar array panels, and a radiator panel, all attached to a connecting cube by Marmon band clamps. The width of the model is 348.6 in. and the overall length is 144.3 in. Other principal dimensions of the model are shown in the schematic of Fig. 2. All of the major components are made from 6061-T6 aluminum. A detailed description of the experimental model is given in Ref. 7.

Received March 24, 1986; presented as Paper 86-0838 at the AIAA/ASME/ASCE/AHS 27th Structures, Structural Dynamics and Materials Conference, San Antonio, TX, May 19-21, 1986; revision received Aug. 29, 1986.

*Aerospace Engineer, Structural Dynamics Branch, Structures and Dynamics Division. Member AIAA.
†President. Member AIAA.

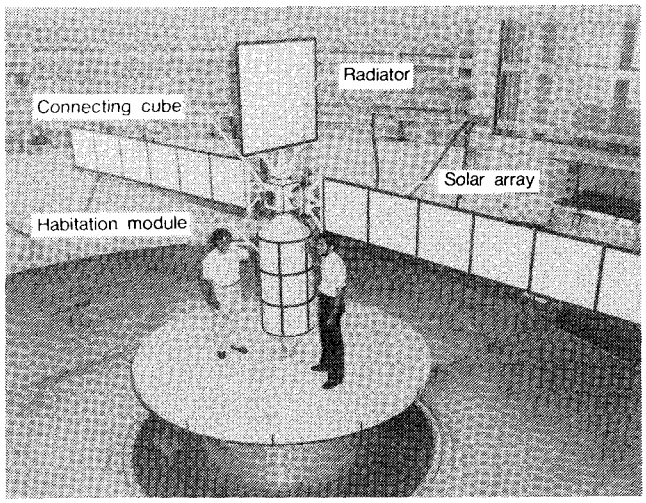

Fig. 1 Assembled generic dynamic model.

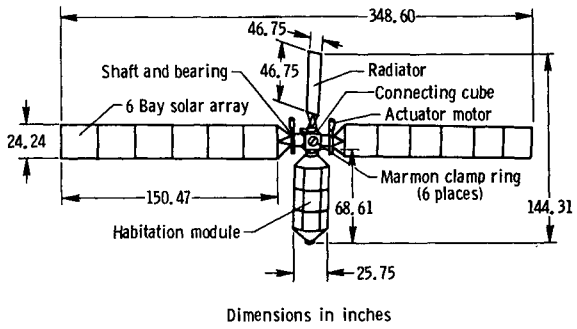

Fig. 2 Dimensions of generic model.

Design of the substructure dimensions and stiffness was based on the expected vibration frequencies of scaled space station models. Although no scale factor could be chosen in the absence of a full-scale design, the frequencies of full-scale components has been estimated by preliminary calculations as shown in Ref. 8. The fundamental flexible body frequencies of full-scale components are estimated to be within one order of magnitude of the following: habitation module ≈ 10 Hz, radiator panel ≈ 1.0 Hz, and solar array panels ≈ 0.1 Hz. To simulate a dynamically scaled model, vibration frequencies of the generic model were increased in inverse proportion to a scale factor of 1/10. Thus, substructure frequencies in the range of one order of magnitude greater than full scale were designed.

The habitation module is a stiff substructure ($f_1 \approx 100$ Hz) relative to the radiator and solar array panels. The radiator panel is a structure of moderate stiffness ($f_1 \approx 10$ Hz), whereas the solar array panels are quite flexible ($f_1 \approx 1$ Hz). The solar arrays were constructed with six nearly square honeycomb sandwich panels that were bolted together. This construction allowed the flexibility to add or remove panels to change the frequency of the solar array panels as desired. The connecting cube used to attach the assemblage is very stiff ($f_1 \approx 300$ Hz) relative to the other substructures.

The generic model, the model formed when the substructures are interconnected as shown in Fig. 1, has vibration modes which occur at a frequency of less than 1 Hz. This frequency of vibration was specifically designed into the structure to evaluate the effects of cable suspension and ambient air on flexible structures typical of large space structure dynamic models.

Analysis and Test Methods

Analysis Methods

The engineering analysis language (EAL) finite-element program,[9] was used to predict the vibration modes of the generic model. A schematic diagram of the analytical model, shown in Fig. 3, indicates the degree of grid refinement used. Six analytical models were developed, one for each substructure and one for the assemblage. The generic model was formed by connecting each substructure analytical model at the appropriate interface. Approximately 4000 degrees of freedom were used in the generic model analysis.

In addition to the generic model, suspension cables were modeled in the analysis. The effects of prestress due to gravity loading were included in the vibration analysis to predict cable suspension modes. The cable suspension system illustrated in Fig. 4 was used to suspend each substructure and the generic model. A detailed description of the analytical models may be found in Ref. 7.

Test Methods

The generic model was tested in the NASA Langley Research Center 16 m thermal-vacuum chamber. The model was suspended by two steel cables as shown in Fig. 4. Tests were performed in both air and near-vacuum (9 mm Hg) conditions. Vibration tests to characterize the modal properties and limited static tests to refine portions of the analytical models were performed.

Modal vibration tests were conducted on each substructure as well as the assemblage. The tests were performed by applying sinusoidal, random, and impulse forces to the models and simultaneously measuring the acceleration response at various locations. Servo accelerometers were used to measure the response acceleration and impact hammers and electrodynamic shakers were used as excitation sources. A Hewlett-Packard 5451C computer system was used to acquire and reduce the test data. Frequency response functions were computed and curve fit to extract the modal parameters, namely, natural frequencies, modal damping, and mode shapes. Several excitation locations, input force levels, and response measurement locations were used to obtain the best estimate of modal parameters. Natural frequencies reported herein are repeatable to within $\pm 1\%$. Damping estimates, however, are subject to more error and are discussed in the damping characterization section of this paper. The measured mode shapes were easily matched with predicted modes; however, the orthogonality between measured and predicted mode shapes was not computed.

Substructure Analysis Verification Method

Each substructure was analyzed during the design phase to insure that the model could withstand gravity forces and still be flexible enough to meet the vibration frequency requirements described above. When fabrication drawings were available, the analytical models were refined to account for changes in geometry and/or member sizes dictated by fabrication considerations. Thus, the analysis models were based on engineering fabrication drawings that are considered the best information usually available prior to hardware testing.

Since finite-element techniques were used, the grid refinement could lead to analysis errors. Several grid refinements were evaluated before the grid shown in Fig. 3 was chosen. The grid in Fig. 3 was found to be well converged for the solar array and radiator vibration modes of interest. The fundamental frequency of both the habitation module and the connecting cube remained sensitive to the grid refinement. Fortunately, the fundamental frequency of the habitation module and connecting cube is sufficiently high such that the substructures can be treated as rigid in the frequency range of interest. Thus, further grid refinement of the model shown in Fig. 3 was not necessary.

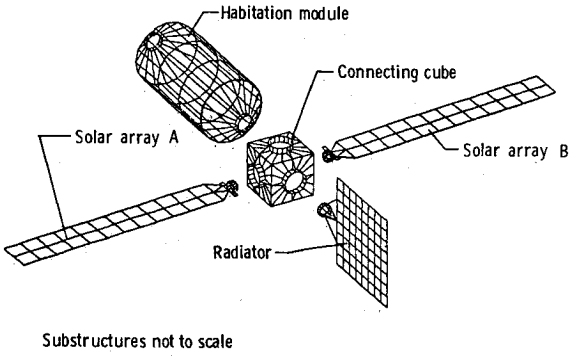

Fig. 3 Finite-element grid used in analytical models.

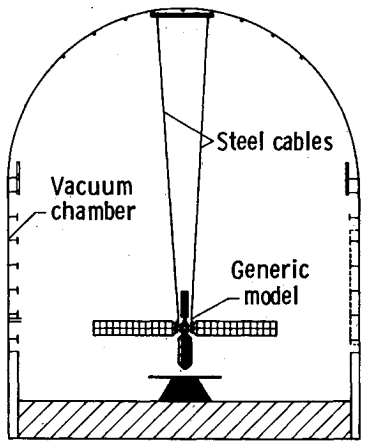

Fig. 4 Schematic diagram of vacuum sphere and generic model cable suspension.

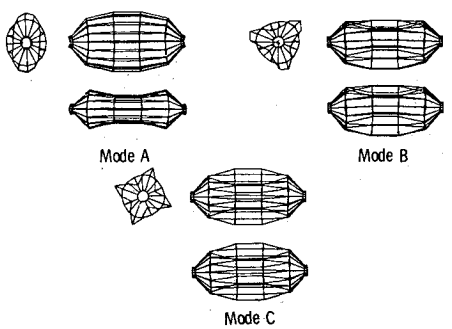

Fig. 5 Habitation module analytical mode shapes.

Connecting Cube and Habitation Module

Dynamic tests of the connecting cube were performed using suspension cables to simulate free-free boundary conditions. The fundamental frequency of the connecting cube exceeded 300 Hz as verified by both test and analysis data. Since the frequency range of interest of the generic model was low, the connecting cube could be modeled with a relatively coarse model. Thus, no changes in the connecting cube analytical model were made.

The habitation module was tested and analyzed to obtain the first few flexible vibration modes. The tests were conducted using two suspension cables. Table 1 gives the experimental and analytical natural frequencies of the habitation module. Analytical mode shapes for the habitation module are shown in Fig. 5. Although the analysis frequencies differ from the test data, the analysis model was not refined. The average 7.8% frequency error was not considered to be significant because of the high frequency of the habitation module relative to the frequency range of interest.

Solar Array Panel

Modal tests of both solar array panels were performed in near-vacuum conditions using a two-cable suspension system. Although attempts were made to fabricate identical panels, slight differences in natural frequencies existed, as shown in Table 2. The average value of the natural frequencies of panels A and B have been used to compare with the solar array analytical model results. The first four solar array panel modes shapes are shown in Fig. 6. Table 3 lists the frequencies from the averaged experiment, initial analysis, and refined analysis. The initial analysis results showed an average 8.1% error in frequency. Since the solar array modes were the dominant low-frequency modes of the generic model, a refinement in the solar array model was desired.

The method for analytical model refinement used herein is based on static test data. As structures become more flexible, structural properties determined from static test data become more accurate. Both the mass and stiffness properties of a structure can be measured statically. The total mass of the solar array was measured and used to refine the mass distribu-

Table 1 Habitation module substructure frequencies

Frequency (Hz)			
Test	Analysis	Percent error	Mode shape
137	143	4.4	A
141	167	18.4	B
177	178	0.6	B
219	203	-7.3	C
221	203	-8.1	C
		Average 7.8	

Table 2 Solar array panel average frequencies

Frequency (Hz)			
Panel A	Panel B	Average frequency	Mode shape
2.00	1.96	1.98	First bending
5.32	5.40	5.36	Second bending
5.73	5.81	5.77	First torsion
11.22	11.17	11.20	Third bending
14.29	14.21	14.25	Second torsion
18.45	18.56	18.50	Fourth bending
23.63	23.69	23.66	Third torsion
27.93	27.96	27.95	Fifth bending
33.86	34.02	33.94	Fourth torsion

Table 3 Solar array panel substructure frequencies

Frequency (Hz)					
Average test	Initial analysis	Percent error	Refined analysis	Percent error	Mode shape
1.98	1.69	-14.6	2.08	5.1	First bending
5.36	5.12	-4.5	5.35	-0.2	Second bending
5.77	5.43	-5.9	6.31	9.4	First torsion
11.20	10.48	-6.4	11.13	-0.6	Third bending
14.25	12.90	-9.5	14.35	0.7	Second torsion
18.50	17.53	-5.2	18.88	2.1	Fourth bending
23.66	21.30	-10.0	24.19	2.2	Third torsion
27.95	26.25	-6.1	28.76	2.9	Fifth bending
33.94	30.33	-10.6	33.22	-2.1	Fourth torsion
		Average 8.1		Average 2.8	

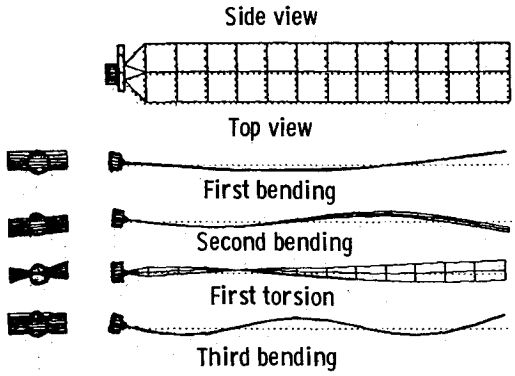

Fig. 6 Solar array panel analytical mode shapes.

Table 4 Radiator panel substructure frequencies

Frequency (Hz)		Percent	
Test	Analysis	error	Mode shape
13.94	14.60	4.7	First torsion
15.21	15.99	5.1	First longitudinal bending
31.69	35.94	13.4	First lateral bending
40.85	44.40	8.7	Second torsion
44.57	44.79	0.5	Second longitudinal bending
	Average	6.5	

Table 5 Generic model frequencies

Mode	Frequency (HZ)		Percent	
number	Test	Analysis	error	Mode shape
1	.052	.053	1.9	Rigid body Z rotation
2	.125	.129	3.2	Rigid pendulum X translation
3	.136	.147	8.1	Rigid pendulum Y translation
4	.353	.324	-8.2	Symmetric X rotation/solar panel bending
5	.750	.757	0.9	Antisymmetric X rotation/solar panel bending
6	1.00	1.01	1.0	Rigid Y rotation
7	1.24	1.29	4.0	First solar panel anitsymmetric bending
8	2.74	2.84	3.6	Second solar panel symmetric bending
9	3.81	3.92	2.9	Second solar panel antisymmetric bending
10	4.43	4.88	10.2	Solar panel antisymmetric torsion
11	4.60	4.94	7.4	Solar panel symmetric torsion
12	4.85	5.05	4.1	Radiator bending
		Average	4.6 percent	

tion of the analytical model. The mass was increased to account for paint, bolts, and additional weld area. Uncertainties existed in the stiffness properties of the solar array panel due to the use of sandwiched honeycomb material. Thus, static bending tests were performed to determine the flexibility of the panel.

A backstop fixture was designed to support each substructure in a cantilevered fashion. Point loads were applied to the free end of the solar array panels such that the flexibility of the panels could be measured. Analytical and experimental static deformations were compared and used to adjust the effective honeycomb stiffness in the analytical model. The solar array analytical model, refined based on static test data, was used to compute the vibration frequencies shown in Table 3. The refined analysis indicates an average frequency error of 2.8%. The refined solar array analysis model was incorporated into the generic analytical model.

Radiator Panel

Dynamic analysis of the radiator panel indicated several torsion and bending modes. Modal tests of the radiator panel were performed using a two-cable suspension. Table 4 lists the experimental and analytical radiator panel frequencies and Fig. 7 shows the mode shapes of the first four flexible modes of the radiator. An average 6.5% error occurred between the predicted and experimental frequencies. Since the assemblage modes of interest were dominated by solar array deformations, no further refinement of the radiator model was felt necessary.

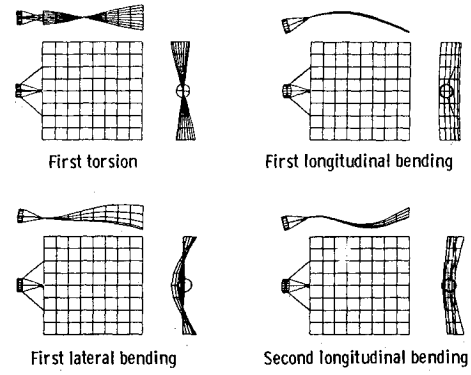

Fig. 7 Radiator panel analytical mode shapes.

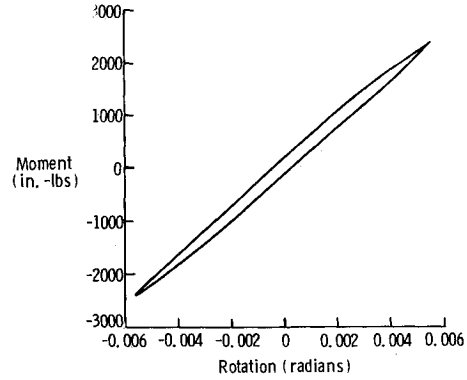

Fig. 8 Marmon band load-deflection test data.

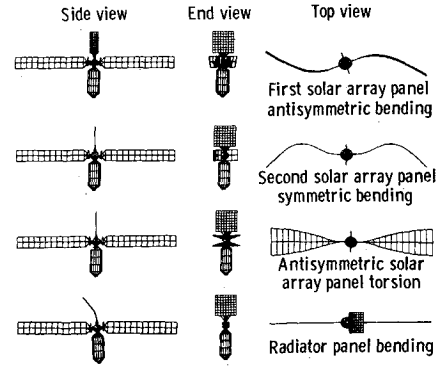

Fig. 9 Typical analytical mode shapes of generic model.

Generic Model Verification Method

The analytical model used to predict the mode shapes and frequencies of the generic model was formed by rigidly connecting the substructure analytical models at the proper interface locations. Since the substructure analytical models were verified through individual substructure tests, the only uncertainty in the assemblage analysis model was the interface joints. The experimental joints are made by connecting the

substructures with a Marmon band clamp. To determine the integrity of the experimental joint, static tests of the Marmon band were performed.

Load-deflection data on the Marmon band were obtained by clamping the band to a backstop fixture and loading the opposite side of the band. A bending moment was applied to the Marmon band and the relative rotation across the band was measured. Typical load-deflection behavior of the Marmon band is shown in Fig. 8. The Marmon band stiffness was linear with little hysterisis. The data of Fig. 8 indicates a bending stiffness of 4.6×10^5 in.-lb/rad, which was found to be sufficient to act as a rigid link between the flexible solar array panels and the connecting cube.

Dynamic analysis was performed to compute the first 12 modes of the cable suspended generic model shown in Fig. 1. Vibration tests were performed to determine modal parameters for the first 12 modes. Table 5 presents the experimental and analytical frequencies for the generic model and Fig. 9 shows typical mode shapes. The analytical and experimental frequencies differ by an average of 4.6%.

A comparison of analytical and experimental natural frequency is generally accepted as a valuable tool in verifying an analytical model. The accuracy required in dynamic analysis depends on the use of the analysis. Dynamic response predictions for active vibration control may require very accurate analytical models, whereas other analytical predictions may suffice with less accurate knowledge of vibration frequencies and mode shapes. For built-up structures such as the generic model described herein, frequency agreement within 5% is reasonable. Should higher accuracy be required, further refinement of analytical models using additional static test data can be performed. The advantage of using static test data to refine analytical models is that the refinement is made in the physical coordinates, which results in a completely consistent analysis. The increased flexibility of large structures such as the space station enables accurate structural properties to be derived from static data.

Table 6 Cable suspended and free-free frequencies of the generic model

Mode number	Frequency (Hz) Cable suspended	Free-free	Mode shape
1	.053	0.0	Rigid body Z rotation
2	.129	0.0	Rigid pendulum X translation
3	.147	0.0	Rigid pendulum Y translation
4	.324	0.0	Symmetric X rotation/solar panel bending
5	.757	0.492	Antisymmetric X rotation/solar panel bending
6	1.01	0.0	Rigid Y rotation
7	1.29	1.31	First solar panel antisymmetric bending
8	2.84	2.87	Second solar panel symmetric bending
9	3.92	3.94	Second solar panel antisymmetric bending
10	4.88	4.87	Solar panel antisymmetric torsion
11	4.94	4.93	Solar panel symmetric torsion
12	5.05	5.08	Radiator bending

Table 7 Ambient air effects on generic model frequencies and damping

Mode number	Frequency (Hz) Vacuum	Air	Percent decrease	Critical damping ratio (C/C_c %) Vacuum	Air	Percent increase
4	0.353	0.34	3.7	0.53	0.75	42
7	1.24	1.21	2.4	0.20	0.27	35
8	2.74	2.64	3.7	0.14	0.20	43
9	3.81	3.71	2.6	0.09	0.12	33
10	4.43	4.35	1.8	0.27	0.28	3.7
11	4.60	4.40	4.3	0.21	0.25	19
		Average	3.1		Average	29

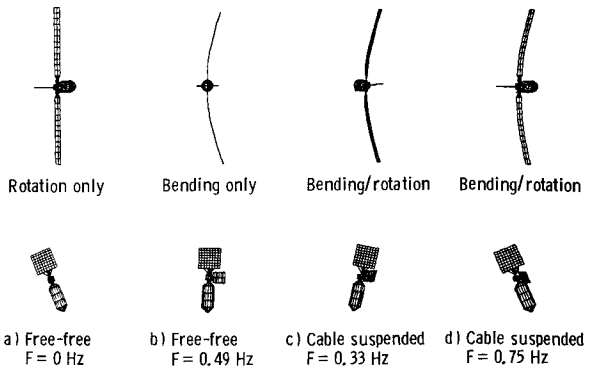

Fig. 10 Analytical shapes of modes 4 and 5: free-free and cable suspended.

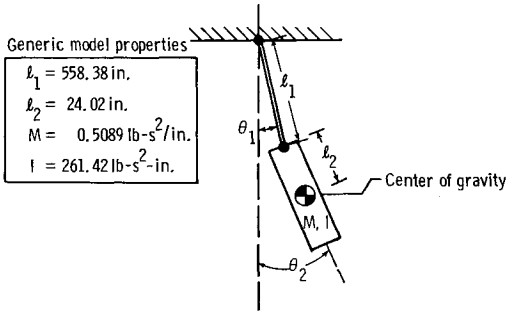

Fig. 11 Schematic diagram of double pendulum.

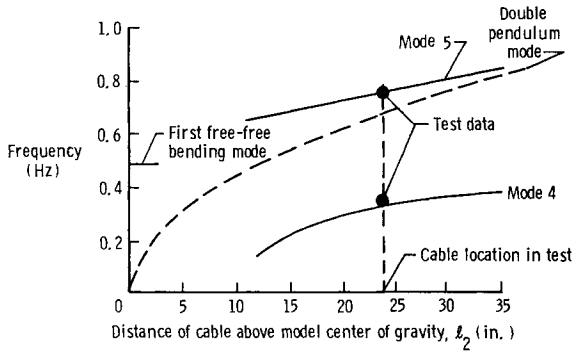

Fig. 12 Effect of cable to model attachment location on frequency.

During the analytical model verification process, the analysis must include the effects of the suspension system used in the ground vibration tests. Since free-free vibration characteristics of spacecraft are sought, the verified analysis model must be modified to remove the suspension system effects. The next section describes some important effects of the cable suspension systems on the vibration characteristics of structures.

Suspension Cable Effects

Cable suspension systems are frequently employed to support structures during ground vibration tests. Structures which exhibit high natural frequencies relative to cable pendulum mode frequencies are not significantly affected by the cables. Reference 4 describes a number of cable suspension systems and their effect on model vibrations. Reference 5 shows that the length of the suspension cables can be adjusted to separate the frequency of the fundamental pendulum mode from that of the first flexible model mode. A generally accepted criterion is to maintain the ratio between the model frequencies of in-

terest to pendulum mode frequencies ≥ 5. If this ratio of frequency separation is maintained, the cable suspension has been found to have little effect on the model vibrations.

The generic analytical model has been used to study the effect of the cable suspension used during the test program. Table 6 shows the predicted generic model frequencies for the cable suspended and free-free configurations. Modes 1-3 and 6 are rigid-body modes, since the mode shapes involve no flexible deformation of the model and the free-free analysis predicts a zero frequency. Modes 7-12 show only small changes in frequency when analyzed with or without cables. Modes 4 and 5 required further investigation.

The free-free analysis predicted modes 4 and 5 to be a rigid-body rotation about the model center of gravity (Fig. 10a) and a symmetric bending mode of the solar array panels (Fig. 10b). Analytical results with cable suspension, however, predicted two modes that exhibit both rotation and bending of the generic model (Figs. 10c and 10d). The suspension cables coupled the rigid-body rotation mode and the solar array bending mode. The coupling is due to a double pendulum mode (rotation about the model center of gravity) of nonzero frequency. To better understand this mode, the schematic shown in Fig. 11 can be used. A massless rigid link of length ℓ_1 (representing the suspension cable) is shown connected to a second link (representing the model) with mass M, inertia I, and length parameter ℓ_2. The length ℓ_2 is distance from the center of gravity of link 2 to the interface between links 1 and 2.

Two modes of vibration of the mechanism of Fig. 11 exist. The first mode involves nearly equal rotations of the cable and model, $\theta_1 \approx \theta_2$. A second mode exists where $\theta_1 \neq \theta_2$, which produces a rotation of the model about its center of gravity, often called the double-pendulum mode. To compute the frequency of these two modes, the following equation may be used:

$$\begin{bmatrix} g\ell_1 M & 0 \\ 0 & g\ell_2 M \end{bmatrix} \begin{Bmatrix} \theta_1 \\ \theta_2 \end{Bmatrix} - \omega^2 \begin{bmatrix} \ell_1^2 M & \ell_1\ell_2 M \\ \ell_1\ell_2 M & \ell_2^2 M + I \end{bmatrix} \begin{Bmatrix} \theta_1 \\ \theta_2 \end{Bmatrix} = \begin{Bmatrix} 0 \\ 0 \end{Bmatrix} \quad (1)$$

Using the properties for the generic model given in Fig. 11, the two frequencies predicted by Eq. (1) are $f_1 = 0.129$ Hz and $f_2 = 0.640$ Hz.

The first mode, f_1, corresponds to mode 2 in Table 4, which is a simple pendulum mode. The second mode predicted by Eq. (1) is the mode that couples with the solar array bending mode. This double-pendulum mode is not sufficiently separated in frequency from the generic model bending mode to prevent coupling. The double-pendulum mode frequency is sensitive to the parameter ℓ_2, the distance from the model center of gravity to the cable attachment location. The dashed curve of Fig. 12 shows the change in frequency of the double pendulum mode as the parameter ℓ_2 is varied. When the cable is attached at the model center of gravity, $\ell_2 = 0$, the frequency of the double-pendulum mode is zero. As the distance from the cable attachment location relative to the model center of gravity is increased, the frequency of the double-pendulum mode increases. The double-pendulum mode couples with the free-free bending mode to form modes 4 and 5. The solid curves of Fig. 12 show modes 4 and 5 of the generic model to also be altered by the cable attachment location. The solid curves are generic analytical model results and the two solid symbols represent the experimental results. These data indicate accurate modeling of cable attachments must be performed to verify analytical models based on ground vibration test data.

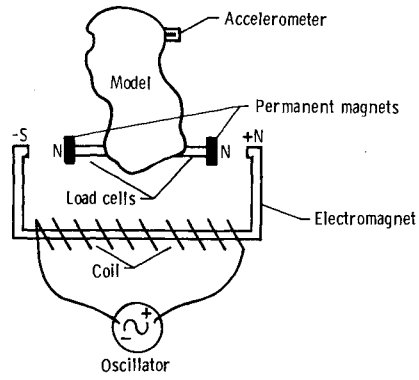

Fig. 13 Schematic diagram of noncontacting electromagnet shaker used in damping study.

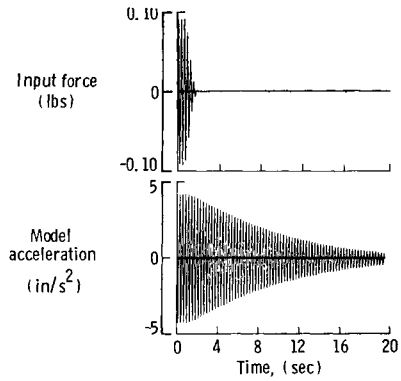

Fig. 14 Typical input force and model acceleration transient time histories.

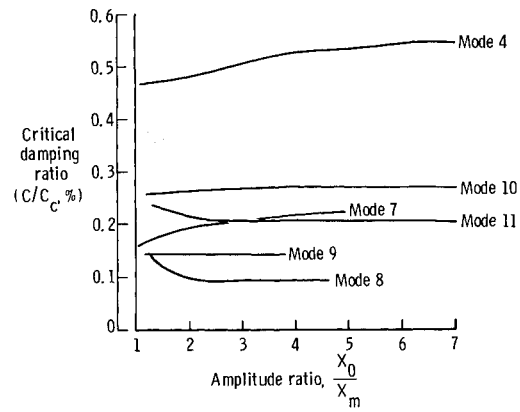

Fig. 15 Amplitude-dependent damping of generic model.

Damping Characterization

In addition to frequencies and mode shapes, damping information is required to more fully characterize the dynamics of a structure. Modal damping is usually measured experimentally, since few analysis methods are available to predict damping. Both frequency domain and time domain methods of measuring damping are available. Damping characterization by frequency domain methods is performed by direct measurement from a frequency response function or by curve fitting frequency response functions. Time domain methods often use

logarithmic decrement or multimode curve fitting techniques to estimate damping.

Damping characterization of the generic model was performed by all of the aforementioned methods. The logarithmic decrement method proved to be the most reliable and repeatable method. The critical damping ratio C/C_c for each mode was computed by the equation

$$C/C_c = m/2\pi \ell n(X_0/X_m) \quad (2)$$

where X_0 is an initial vibration amplitude and X_m an amplitude after m cycles.

Figure 13 shows the modal damping exhibited by modes 4 and 7–11 as described in Table 5. For most modes, the damping ratio changes as the amplitude of vibration changes, which indicated the presence of amplitude-dependent damping such as friction.

Damping characterization using the logarithmic decrement method is an excellent means of determining damping nonlinearity provided the modes can be excited individually. Several excitation techniques were evaluated and the most successful was an electromagnet exciter. Figure 14 shows a schematic diagram of the noncontacting exciter used in the damping tests. When driven by an oscillator, the electromagnet produced a push-pull effect on two permanent magnets mounted on the model. The oscillator frequency would be set to the natural frequency of the mode desired and then turned off to obtain a free decay as shown in Fig. 15. The excited force rapidly approached zero as the magnetic field collapsed. The noncontacting shaker permitted the modes to be excited independently without adding damping to the structure.

The repeatability of damping measurements is more difficult than frequency measurements. The damping data computed using the logarithmic data was repeatable to $\pm 10\%$. Characterization of generic model damping was much less repeatable using the frequency domain methods described above.

Temperature, humidity, and other atmospheric effects can alter the damping between tests. Thus, it is desirable to test in vacuum conditions if available. To evaluate the effects of ambient air, frequency and damping measurements were taken in air and in near-vacuum (9 mm Hg) conditions. Table 7 lists the frequency and damping for modes 4 and 7–11 in air and in vacuum. The damping values tabulated are averaged to obtain a linear estimate of the nonlinear damping. The frequencies of the modes were lower when ambient air was present by an average of 3.1%. This may be attributed to the effective mass of the air. The modal damping increased when ambient air was present by an average 28% because the air acts as a viscous fluid, which dissipates energy. Extrapolating the ambient air effects to other scale model sizes will require further study. Nevertheless, the data obtained herein indicate that ambient air can produce substantial changes in dynamic properties for panel-type structures.

Conclusions

A generic model was analyzed and tested to evaluate dynamic analysis and experiment methods for characterizing the modal parameters in large multibody space structures such as the space station. Finite-element analysis was used to predict the substructure and generic model dynamic behavior. Static and dynamic tests were performed to refine and verify the analytical models. Coupling between the cable suspension and the model was identified and a method for damping characterization of lightly damped structures using noncontacting exciters was developed. The effects of ambient air on model frequencies and damping were also measured.

Static and dynamic test data should be used to verify substructure analysis models. Structural properties derived from static test data become more accurate as the structure flexibility increases. Verification of analytical models on a substructure level reduced the uncertainty of the generic model analysis. The solar array substructure, when refined using static test data, reduced the average frequency error from 8.1% error to 2.8%. Correlation between experimental and analytical data of the generic model indicated an average frequency error of 4.6%. To obtain good agreement between the analytical and experimental results, modeling of the cable suspension was necessary. Coupling between cable pendulum modes and flexible structure modes occurred due to a double-pendulum effect Analytical results show the level of coupling could be altered by adjusting the cable-to-model attachment location relative to the model center of gravity.

Damping characterization by logarithmic decrement methods enable nonlinear damping to be identified. A noncontacting electromagnet exciter was used to excite individual modes without adding parasitic damping. Damping measurements were significantly influenced by the presence of ambient air. An average 28% increase in damping was exhibited by the generic model when ambient air was present. Mass effects due to ambient air reduced the average generic model vibration frequencies by 3.1%. Further study is required to develop methods for extrapolating ambient air effects to other size models.

References

[1]Berman, A. and Flannelly, W. G., "Theory of Incomplete Models of Dynamic Structures," *AIAA Journal,* Vol. 9, Aug. 1971, pp. 1481–1487.

[2]Berman, A. et al., "Improvement of Analytical Dynamic Models Using Model Test Data," AIAA Paper 80-0800, May 1980.

[3]Link, M., "Identification of Physical System Matrices Using Incomplete Vibration Test Data," *Proceedings of 4th International Modal Conference,* Los Angeles, Feb. 1986, pp. 386–393.

[4]Herr, R. W., "Some Cable Suspension Systems and Their Effects on the Flexural Frequencies of Slender Aerospace Structures," NASA TN D-7693, Sept. 1974.

[5]Hanks, B. R. and Pinson, L. D., "Large Space Structures Raise Testing Challenges," *Astronautics and Aeronautics,* Vol. 21, Oct. 1983, pp. 34–40.

[6]Housner, J. M., "Structural Dynamics Model and Response of the Deployable Reference Configuration Space Station," NASA TM-86386, May 1986.

[7]Belvin, W. K. and Edighoffer, H. H., "Experimental and Analytical Generic Space Station Dynamic Models," NASA TM-87696, March 1986.

[8]Livingston, L. E., "Space Operations Center: A Concept Analysis," NASA TM-81062, Nov. 1979.

[9]Whetstone, W. D., "EISI-EAL Engineering Analysis Language Reference Manual," *EISI-EAL System Level 2091,* Vols. 1 and 2, Engineering Information Systems, Inc., San Jose, CA, July 1983.